私 立 東 海 大 學

資 訊 工 程 研 究 所

碩士論文

指導教授：黃 育 仁 博士

三維高解析血流都卜勒超音波之乳房腫瘤血管研究

3D High-Definition Flow Power Doppler Sonography Studies

of Breast Tumors using Vascularization Evaluation

研究生：連　怡　斌

中　華　民　國　一　百　年　六　月

摘　要

乳癌在婦女的癌症發生率中極高，每年約有上千名婦女因乳癌病逝，乳癌是婦女健康的重大威脅之一，早期發現乳癌可早期進行治療，可降低乳癌的死亡率。在腫瘤的發展過程中，血管新生(angiogenesis)扮演著非常重要的角色。一般常用檢查乳癌的工具有乳房 X 光攝影、核磁共振造影、超音波等。其中乳房 X 光攝影結果雖然精確，卻有高放射劑量的缺點，而核磁共振造影則是成本太高。超音波影像雖然雜訊較多，然而卻有低放射性、成本便宜等優點，加上近年來超音波對乳房組織的解析度不斷提高，因此乳房超音波早已成為乳房檢查重要的工具。

腫瘤周圍血管在腫瘤的生長中扮演著一個非常重要的腳色，血管新生現象被普遍運用來做為觀察腫瘤狀態的依據。高解析血流(high-definition flow, HDF)是一項新的都卜勒超音波技術，對於檢查乳房腫瘤而言，HDF 都卜勒超音波除了能發現腫瘤的形狀，也能偵測血流的強度與方向。對於醫生診斷來說，腫瘤血流資訊已成為不可或缺的資訊。本研究的主旨是希望基於血管新生的現象，透過腫瘤周圍的血流資訊所構建出的三維血管模型，來計算化療前後的血管特徵，並利用這些特徵在早期的療程之後就能預測化療最終的成效，藉此來減少輔助化療帶與病患身體上的痛苦和金錢的花費。在本研究中利用六個血流資訊的量化的特徵、三個形態學處理的特徵和兩個血流方向統計學量化的特徵，與各個階段的化療階段比較之間的變化，來做為預測的依據。

關鍵字：乳房腫瘤，腫瘤血管，血管新生，輔助化療，高解析血流超音波，三維細線化

Abstract

According to American Cancer Society (ACS) statistics, breast cancer is the most common cancer among women in USA. It is the second leading cause of cancer death in women. Tumor vascularization has been proved to be an important factor that correlated with tumor malignancy. Angiogenesis is widely accepted as a process for the growth of cancers. In this study, high-definition flow (HDF) power Doppler ultrasound (US) is performed to investigate blood flow and solid directional flow information in breast tumors. The vascularization of tumor would be used as a factor to estimate the effect of the neo-adjuvant chemotherapy prior to surgery. This study aims to evaluate vascularity changes in three-dimensional (3D) HDF power Doppler ultrasound images during neo-adjuvant chemotherapy of breast cancer in patients. The proposed method utilizes 3D Gaussian lowpass filter to reduce the noise and speckles and applies a 3D thinning algorithm for extracting vascularity centerlines. The color of voxel within the HDF Doppler sonography indicates the direction information of blood flow in the vascular centre-line. In this study, six vascularity quantization features, three morphological features and two vascular direction features are extracted for evaluate the correlation between the vascularity changes and neo-adjuvant chemotherapy effect.

Keywords: breast tumor, tumor vascularization, Angiogenesis, neo-adjuvant chemotherapy, HDF power Doppler ultrasound, 3D thinning

INDEX

LIST OF FIGURE

LIST OF TABLES

CHAPTER1

INTRODUCTION

Breast cancer is one of the most serious cancers for women. According to American Cancer Society (ACS) statistics, breast cancer is the most common cancer among women in USA. It is the second leading cause of cancer death in women, after lung cancer. Early diagnosis and early treatment is the most effective way of reducing mortality caused by breast cancer. In this decade, neo-adjuvant chemotherapy could substantially improve disease-free and overall survival for the most part of patients. The treatment procedure was used to shrink the tumor volume and to reduce the probability of a relapse after surgery. However, the treatment period was not necessarily obtaining an apparent effect for all patients. About 20% to 30% of patients showed either no or poor response to chemotherapy [1]. Due to patients suffer great pain during the period of adjuvant chemotherapy, finding a method to early predict the tumors response of neo-adjuvant chemotherapy is needed.

Angiogenesis has been shown to play a key role in the transition of tumors for the establishment, growth and dissemination. It is widely accepted that vascularity of a tumor represents an important factor that correlated with tumor malignancy [2,3]. The growth of breast cancer is equally connected to angiogenesis during the development of the tumor. Therefore, tumor vascularity is an important factor that correlated with tumor malignancy. The Doppler ultrasound blood flow signals have been demonstrated that associated with malignant tumor vascularization. Power Doppler ultrasound was developed to improve the visualization of small vessels by using a different measurement of the strength of the Doppler signal which fundamentally depends on the amount of blood. 3D power Doppler breast ultrasound

can be used to assess the vascularization of the whole tumor, instead of the limited transverse and longitudinal planes in 2D Doppler ultrasound. Moreover, high-definition flow (HDF) Doppler ultrasound was performed to investigate blood flow and solid directional flow information in breast tumors. The vascularization of tumor would be used as a factor to evaluate the effect of the neo-adjuvant chemotherapy prior to surgery.

In this study, information about tumor and blood vessels, included voxel of tumor, vascularity and direction of blood flow, were extracted from 3D HDF Doppler sonography. Firstly, the region of tumors was selected by experienced experts and a preprocessing including Gaussian filter and morphology methods was performed. A 3D six-subiteration thinning algorithm was used to generate blood vessel trees. Then all information surrounding the tumor region which dilated the tumor boundary (3mm) are extracted to evaluate the correlation between the vascularity changes and neo-adjuvant chemotherapy effect. In this study, six vascularity quantization features, three morphological features and two vascular direction features were used to evaluate neo-adjuvant chemotherapy effect. The flowchart of the proposed scheme is shown in Fig. 1. The variation of the vascular features might be useful information as early predictors for physicians to prognose the responses of neo-adjuvant chemotherapy. Early treatment prediction using the 3D HDF Doppler ultrasound could diminish the unnecessary chemotherapy treatments for the patient who had poor response to certain chemotherapy strategies.

In this thesis, Chapter 2 described important binary mathematical morphology operations and structure element. The methods of noise reduction and vascular centerline extraction were proposed in Chapter 3. The results of extracted features were shown in Chapter 4. Chapter 5 gave discussion and conclusion of the tendencies of the features of the 3D HDF Doppler ultrasound imaging.

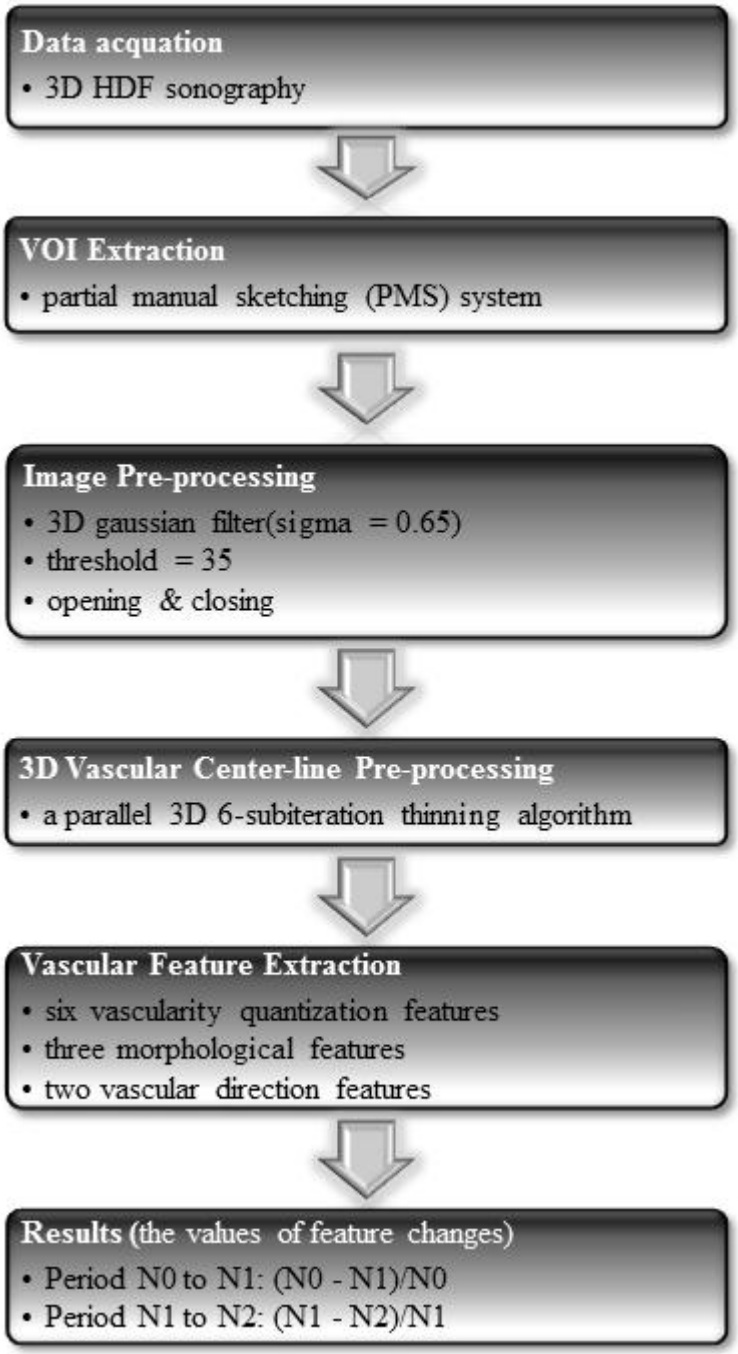

Figure 1. Flowchart of the proposed scheme

CHAPTER 2

MATHEMATICAL MORPHOLOGY

The principle of mathematical morphology is the set theory [4]. Morphology offers a unified and powerful approach as such to various image processing problems. Mathematical morphology has already been widely used in image processing and provides two basic operations, i.e. dilation and erosion.

This study utilized 3D binary mathematical morphology to enhance the 3D HDF Doppler ultrasound imaging. The morphological operators are derived from two-dimensional (2D) binary mathematical morphology. Important binary mathematical morphology operations and structure element were described as follows.

2.1 Opening and Closing

The basic effect of opening is to smooth the contour of an object, breaks narrow isthmuses and eliminates thin protrusions, and closing generally fuses narrow breaks and long thin gulfs, eliminates small holes and fills gaps in the contour. Opening and closing removes small holes in the foreground, changing small islands of background to the foreground. The opening of a set A by a structure element B, denoted as $A \circ B$, is defined as

$$A \circ B = (A \Theta B) \oplus B, \tag{1}$$

where Θ and $\oplus$ denote erosion and dilation[5], respectively. The closing of a set A by a structure element B, denoted as $A \bullet B$, is defined as

$$A \bullet B = (A \oplus B) \Theta B. \tag{2}$$

Thus, the opening A by B is the dilation of the erosion of a set A by B, and the

closing *A* by *B* is the erosion of the dilation of a set *A* by *B*. Figure 2 explain the principle of opening and closing. The 3D opening or closing of a 3D object was also derived from 2D by a 3D structure element as shown in Fig. 4(b).

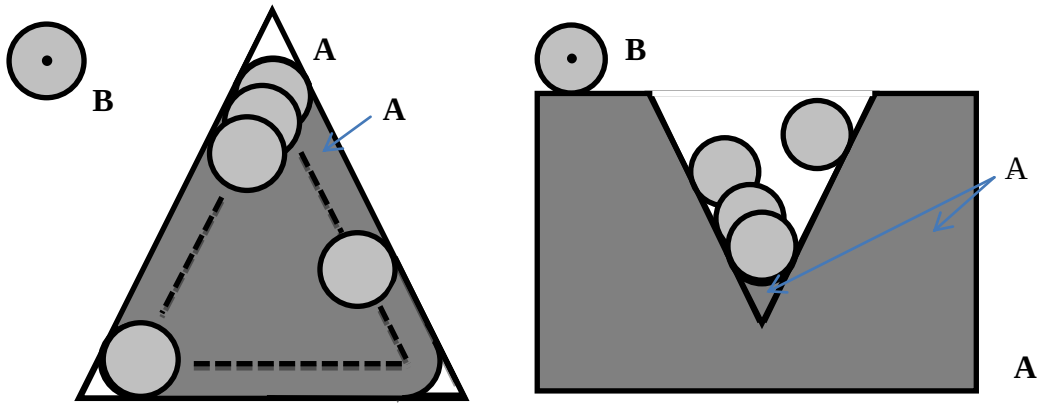

(a) (b)

Figure 2. Structuring element B "rolling" along the inner boundary of A (the dot indicates the origin of B): (a) The dark gray area is the complete opening area; (b) The dark gray area is the complete closing area

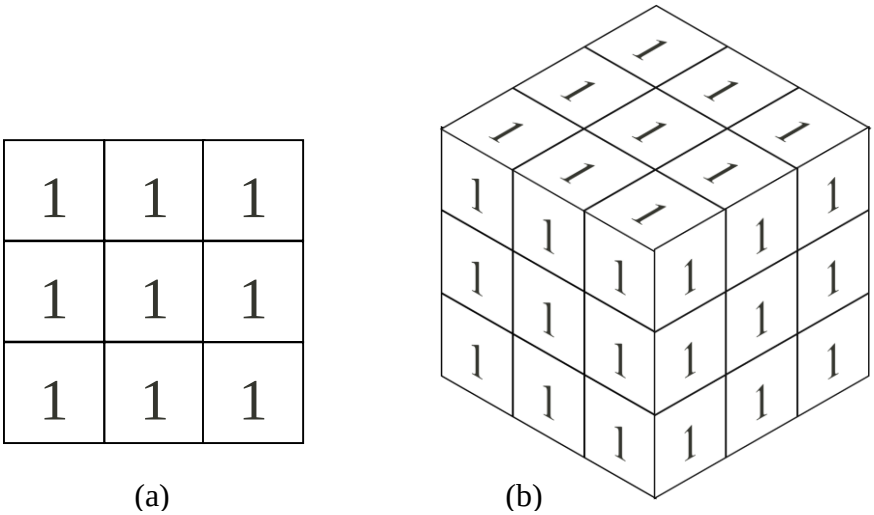

(a) (b)

Figure 3. Structure elements for binary mathematical morphology: (a) 3 × 3 square structure element; (b) 3 × 3 × 3 cube structure element

2.2 Thinning

The thinning methods attempt to obtain a centerline by iteratively removing points, which fit at least one of a sequence of structure elements, from the boundary of an object in images. The thinning operator set out to from the object's boundary and continues inward until no more simple points can be removed. This study utilized a parallel 3D 6-subiteration thinning algorithm [6] to thin the 3D HDF Doppler ultrasound imaging. The detailed descriptions about the 3D 6-subiteration thinning are given in following chapter. Figure 5(b) illustrates the result from Fig. 5(a) by thinning.

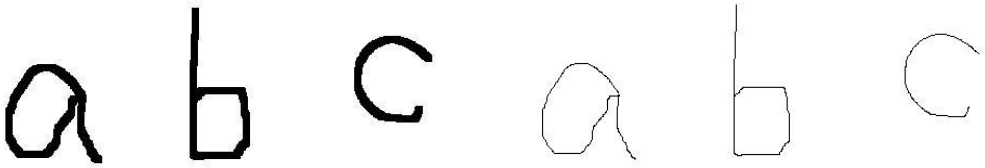

(a) (b)

Figure 4. An example of the result of thinning: (a) Original image; (b) the thinning result of (a)

CHAPTER 3

MATERIALS AND METHODS

3.1 Data Acquisition

3.1.1 Patients and chemotherapy

Patients were recruited into this study consecutively from July 2007 to Oct 2010. Thirty two consecutive T2 breast cancer (Tumor size > 2cm and ≤ 5cm) patients, who received neo-adjuvant chemotherapy were recruited for this study. The diagnosis of breast cancer was made by core needle biopsy. Pre-operative intravenous chemotherapy was given for six courses in each patient and three weeks per cycle. Epirubicin (Pharmorubicin, Pfizer Pharmaceuticals, New York City, NY, USA) 80-90 mg/m2, cyclophosphamide 500 mg/m2 and 5-Fluorouracil 500 mg/m2 on day 1 every three weeks. Sonographic examinations were done (period N1-N6) by using 3D power Doppler ultrasound with the HDF function (Voluson 730, GE Medical Systems, Zipf, Austria, equipped with RSP 6-12 transducer). The period N0 was the sonographic before the chemotherapy.

3.1.2 Sonography acquisition

In this study, sonographic examinations (each lesion included five or six examinations) were done by using 3D power Doppler ultrasound with the HDF function (Voluson 730, GE Medical Systems, Zipf, Austria). A linear-array broadband probe with a frequency of 6–12 MHz, a scan width of 37.5 mm, and a sweep angle of 5◦ to 29◦ to obtain 3D volume scanning was used. Physician kept a fixed sweep angle of 20◦ and power Doppler settings of mid frequency, 0.9 kHz pulse repetition frequency, −0.6 gain, and ‘low 1’ wall motion filter in all cases. All obtained images were stored on the hard disk and transferred to a personal computer using a DICOM

(Digital Imaging and Communications in Medicine) connection for image analysis. Each 3D HDF images contained 155 to 199 2D images, the resolution of each image was approximately 200 × 200 pixels.

3.2 VOI Extraction

An experienced sonography physician who was familiar with breast ultrasound interpretations manually determined 3D contours of the tumor by using a partial manual sketching (PMS) system. The PMS system is identical to virtual organ computer-aided analysis (VOCAL) [7,8] scheme within 4D View software (GE Medical Systems, Zipf, Austria) was performed to obtain an approximated 3D contour. The PMS system estimated 3D contours in the B-mode images by a selectable degree, i.e. 30^{o} or 15^{o}, of rotation. This study performed a very common used rotation degree 30^{o} to define tumor's volume of interest (VOI). Hence six preliminary tumor contours in 0^{o}, 30^{o}, 60^{o}, 90^{o}, 120^{o}, and 150^{o} slice images were manually sketched by the physician. Figure 5 represents the tumor contour manually sketched with each 30◦ rotation. Then the six extracted contours were utilized to build a 3D VOI area for a tumor.

3.3 Image Pre-processing

Due to the 3D HDF Doppler ultrasound images include considerable noises and speckles that make blood vessel identification difficult. Thus preprocessing is a significant issue before extracting vascular centre-lines. An effective preprocessing method for contouring should aim to reduce noises and preserve the useful vascular

information. A 3D HDF ultrasound imaging could be decomposed into three image channels, i.e. B-mode (tumor intensity) channel, blood vessels intensity channel and the direction of blood flow channel. Figure 6 shows images of the three image channels from one slice in a case. The B-mode sonography was used to manually draft tumor volume using the PMS system and Doppler ultrasound imaging (blood vessels intensity channel and direction of blood flow channel) was used for vascular statistical analysis. The morphological features were extracted in blood vessel intensity image. This study performed the 3D Gaussian low-pass filter (with sigma = 0.65) [9] to smooth vascular intensity. The Gaussian filter is a weighted average filter which based on Gaussian function (which also expresses the normal distribution in statistics) for calculating the weighted from the voxels in the mask. The output value of each voxel was generated by its connection neighborhoods. Then a thresholding procedure was performed to convert the HDF Doppler signals into a binary vascular image. A predefined threshold *TH* was set as 35 in this study and the binary vascular image always preserved a satisfied condition of blood vessels. There is no theory supporting *TH* value, but the shape of vascular is most matched in 4D View system that experts use to discuss the 3D HDF US image.

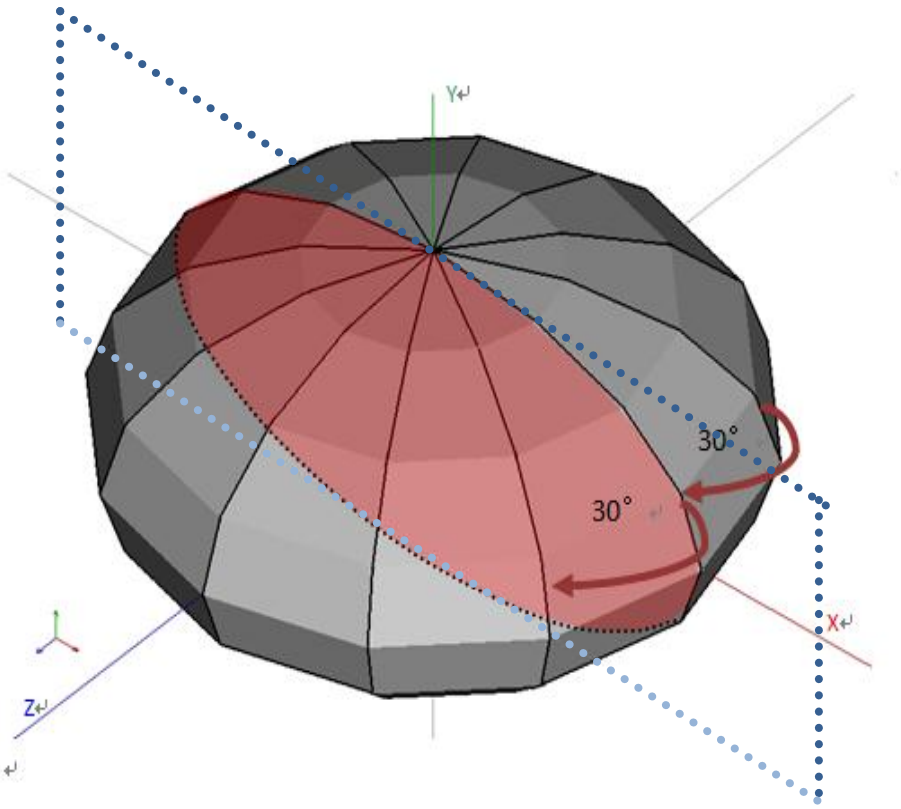

Figure 5. The tumor contour that manually sketched with 30^{o} by experienced physician

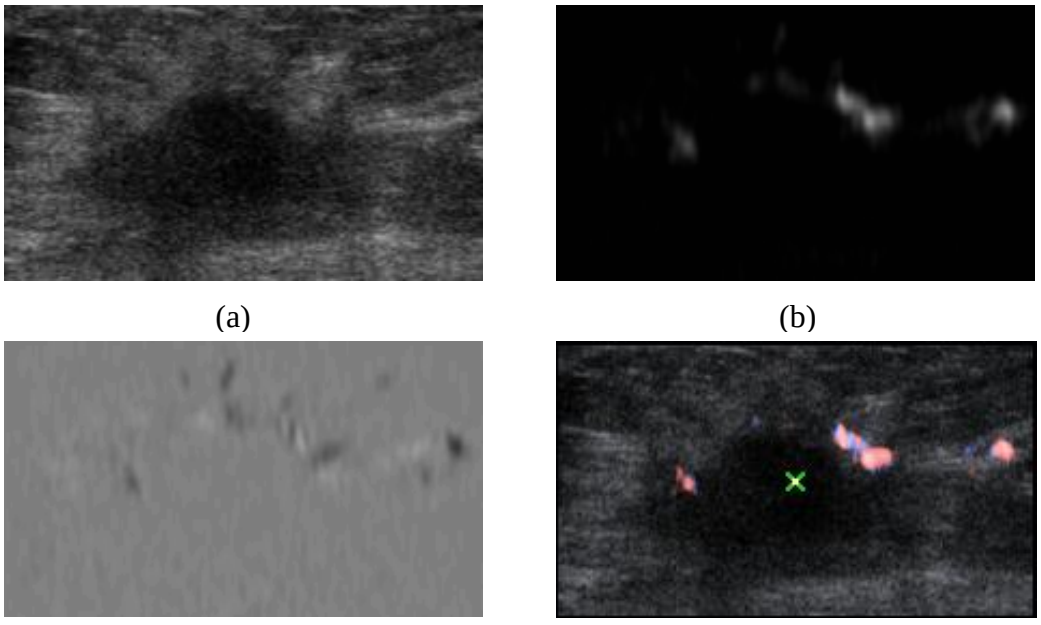

(a) (b)

(c) (d)

Figure 6. (a) B-mode (tumor intensity) channel; (b) blood vessels intensity channel; (c) the direction of blood flow channel; (d) the composed image by using 4D View (slice number 120 of case#13 at period N0)

The binary vascular imaging always contained some cavities on the surface or within the vessels by noise, and some disconnected parts which only one or two voxels between each other (These disconnected regions may a connection blood vessel that only be masked by shadow). The noises and disconnected parts would cause the following 3D blood vessel thinning to generate error skeletons. The proposed method utilized a 3×3×3 cube as a template for the mathematical morphology. A double closing operation, i.e. two successive dilations and then followed by two successive erosions, were started to fill up the 3D vascularity area [10]. In order to delete some small isolated regions which can be considered as speckle, an opening operation was executed. Figure 7 shows the different between original images and preprocessed images.

Moreover, the color of voxel in 3D HDF power Doppler ultrasound imaging represented the direction (0-127 represented that the blood flow moved toward the probe and 129-255 represented that the blood flow moved away the probe) and the intensity represented the speed of blood flow (values of the intensity father away 128 represented the faster speed). Thus the direction information of blood flow would annotate to each point in the vascularity.

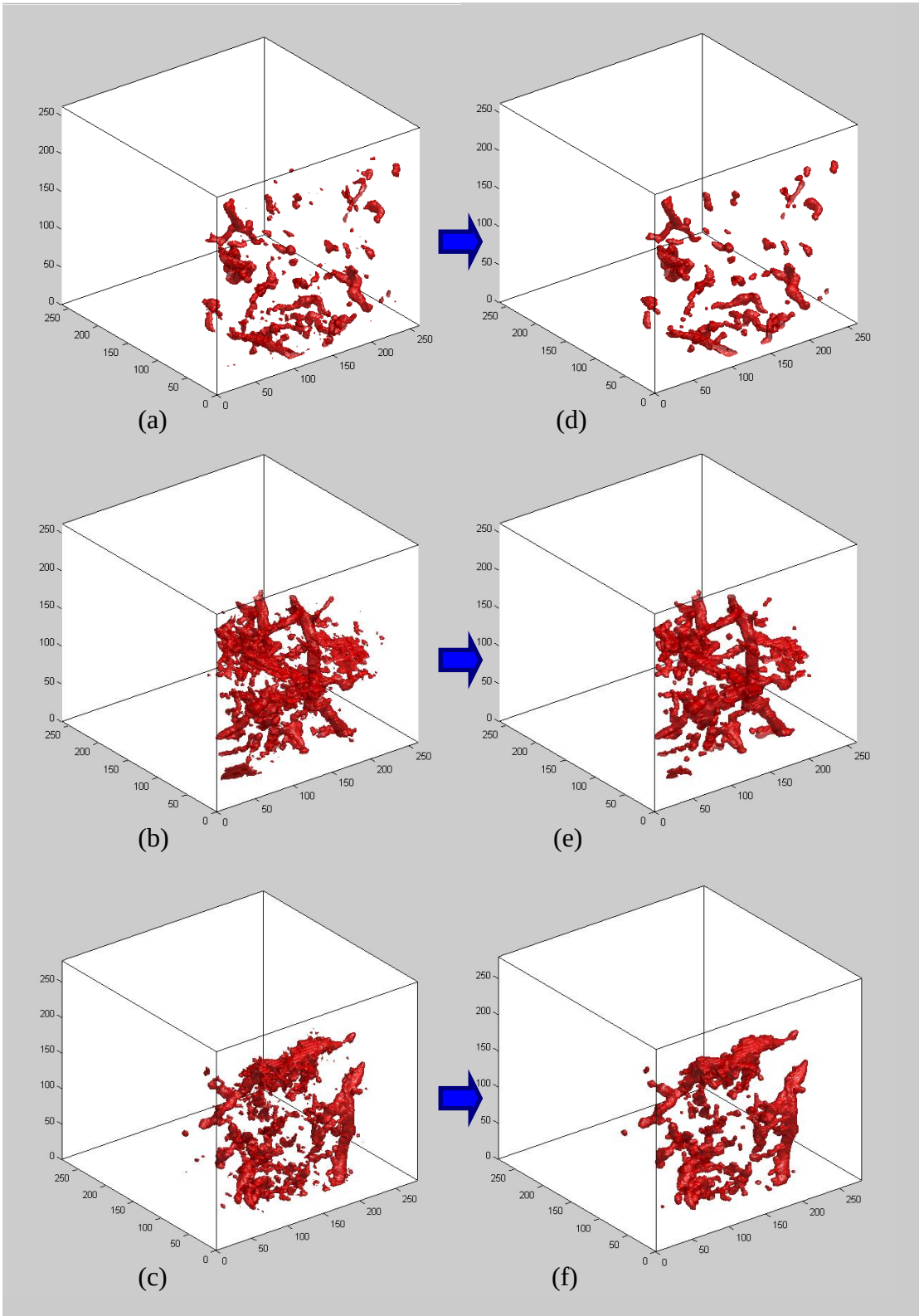

Figure 7. Results of the pre-processing procedure: (a)(b)(c) are the original 3D HDF vascularity images (from left to right: case #12, #15, #23 at period N0); (d)(e)(f) are the corresponding preprocessed images.

3.4 3D Vascular Centre-lines Extraction

Several methods have been proposed for extracting centerline form 3D objects, such as skeletons [11], Potential Field [12], and thinning operators [6,13,14]. The 3D thinning operators attempt to produce a centerline by iteratively removing simple points from the boundary of an object. A simple point is an object point which can be removed without changing the topology of the object. The thinning operator set out to from the object's boundary and continues inward until no more simple points can be removed. The vessel centerline of the 3D vascularity object will be obtained after 3D thinning operator.

This study utilized the parallel 3D 6-subiteration thinning algorithm proposed by Palagyi *et al.* [6] to thin the noise-reduced 3D HDF Doppler ultrasound images. The advantages of the thinning algorithm are that can achieve excellent efficiency and implement easily. By the algorithm the voxel with value 1 is denoted the black point, and the voxel with value 0 is denoted the white point. The algorithm defined a new value of each black points depends on its 3×3×3 neighborhoods. The deletion condition assigned to a subiteration is described by a set of masks or matching templates. A black point is to be deleted if and only if its 3×3×3 neighborhood matches at least one element of the given set of masks. The 3D 6-subiteration thinning algorithm produces either curve skeletons or surface skeletons from 3D binary objects in (26, 6)-connectivity by repetitive iterations until no more points need to be removed. In this study, the algorithm directly extracted vascular centre-lines from elongated 3D binary objects and provided good results and preserved topology. After the thinning algorithm, we deleted the skeleton blood vessels that contained less than four voxels. Figure 8 shows the result of vascular centre-line extraction in a 3D HDF Doppler imaging.

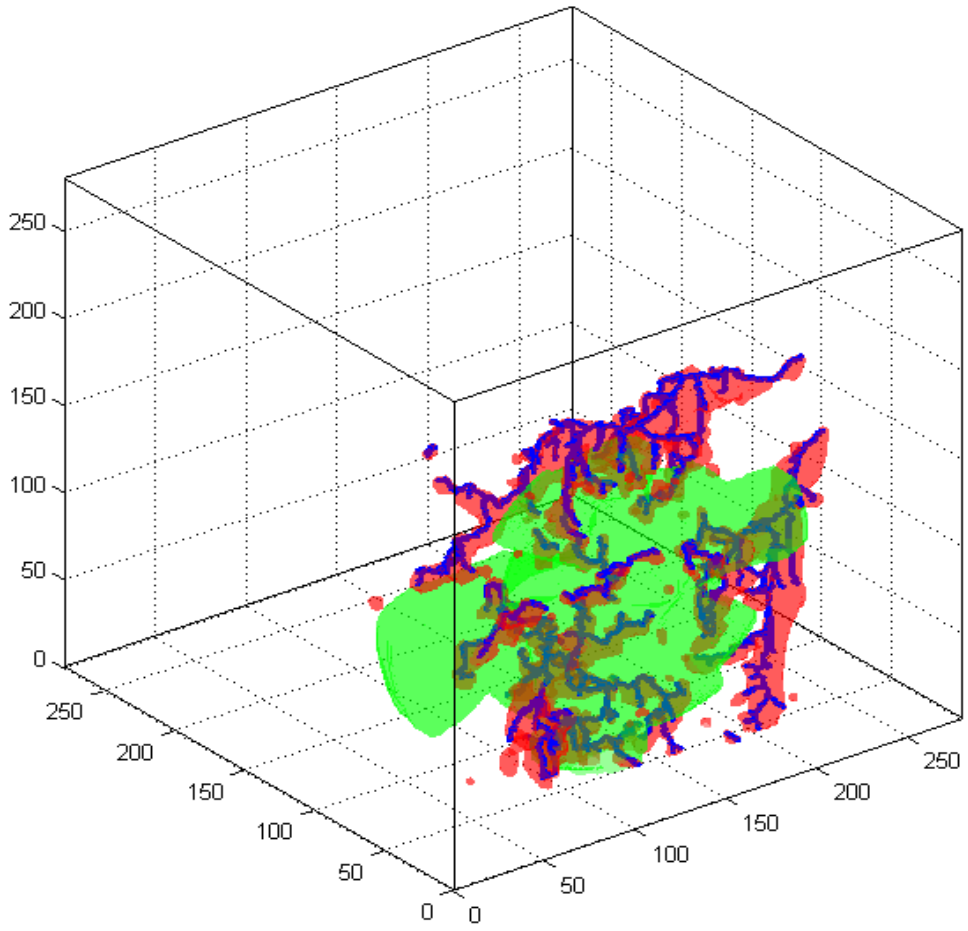

Figure 8. The result of vascular centre-lines extraction (case#23 at period N0): the blue lines are the extracted vascular centre-lines, the red regions are blood vessels and the green area is VOI of tumor.

3.4 Vascular feature extraction

Six vascularity quantization features, three morphological features and two vascular direction features are extracted for evaluate the correlation between the vascularity changes and neo-adjuvant chemotherapy effect.

3.4.1 Vascularity Quantization features

To quantify the HDF Doppler signal, three indices were evaluated from 3-D power Doppler ultrasound. Vascularization index[15,16] denoted *VI*, the ratio between the color voxels (with power Doppler signal). Let *S* denoted the set of all slices in a 3-D power Doppler ultrasound imaging, the *VI* is defined as

$$VI = \frac{\sum_{s \in S} P(s)}{\sum_{s \in S} N(s)}, \tag{1}$$

where $P(s)$ is the number of voxels with power Doppler signal and $N(s)$ is the number of total voxels in the specific area of the slice *s*. Flow index (denoted *FI*), the mean energy per color voxel, represents the average intensity of flow. The *FI* is defined as

$$FI = \frac{\sum_{s \in S} I(s)}{\sum_{s \in S} P(s)}, \tag{2}$$

where $I(s)$ is the intensity sum of voxels with power Doppler signal in the specific area of the slice *s*. Vascularization flow index (denoted *VFI*), the mean color value in all the voxels in the obtained volume, represents both vascularization and flow. The *VFI* for the specific area of the slice *s* is defined as

$$VFI = \frac{\sum_{s \in S} I(s)}{\sum_{s \in S} N(s)}. \tag{3}$$

In this study, a specific area was selected from dilated volume of the 3D

extracted VOI. The dilated volume was the volume of tumor which dilated 3mm. For more precise observation of vascular changes, the vascular quantization features *VI*, *FI* and *VFI* were performed for another specific area. The region of second specific area is inside the tumor and features denoted *iVI*, *iFI* and *iVFI*..

3.4.2 Morphological features

After the vascular trees were constructed, the morphological changes would be explored to identify the characteristics. Let *Cm* is the vascularity centerline matrix. Each point in this matrix stored the result of the 3D images after thinning. Each point in *Cm* was assigned by 255 (belong to centerlines); otherwise the value was 0 (not belong to centerlines), and $Adj(i)$ are the points in the (26, 6)-connectivity of *i*. The total number of branch (denoted *NB*), was the number of branch of vascularity centerlines in *Cm*. A point had three connection in the (26, 6)-connectivity was regarded as a branching point *j*; *j* = 1 when $|Adj(i)| = 2$; otherwise, *j* = 0. The value of $|Adj(i)|$ is the total number of the points in $Adj(i)$. The *NB* is defined as the number of connect region at j = 1. The shortest distance between vessels and the center of tumor (denoted *SDVC*) was the shortest distance between the vascular centerline and the barycenter of tumor. The *SDVC* is defined as:

$$min(\ (Xi\text{-}x)^2\ +\ (Y_i\text{-}y)^2\ +\ (Zi\text{-}z)^2\ ), \tag{5}$$

where (*x*, *y*, *z*) was the coordinate of barycenter and $\forall i \in C_{mi}$ (X_i, Y_i, Z_i) *w*as the coordinate of point *i*. The total number of tree (denoted *NT*) was the number of vascularity centerlines in *Cm*. A connecting region in *Cm* was regarded as a vascularity centerline.

3.4.3 Vascular direction features

In a vascular direction channel, the value 128 is represented the back ground or the direction that perpendicular to the probe, value 1 to 127 represented the speed of flow away the probe and value 129 to 255 represented the speed of flow close to the probe. All the flow direction values in the *xy* slice were made from the intensity histogram statistics (range 1-255). This study calculated the value of histogram to extract vascular direction feature [5].

Let z is a random variable indicating intensity, $p(z)$ is the histogram of the intensity levels in a specific region. The mean intensity μ is shown as

$$\mu = \sum_{i=1}^{L} z_i \, p(z_i) \quad , \tag{6}$$

and the standard deviation *DE* in the image channel is defined as

$$DE = \sqrt{\sum_{i=1}^{L} (z_i - \mu)^2 \, p(z_i)} \quad . \tag{7}$$

Finally the entropy *EN* is a measure of disorder (the higher the entropy, the higher the disorder) for vascular direction. *EN* is defined as

$$EN = -\sum_{i=1}^{L} p(z_i) \log_2 p(z_i) \quad . \tag{8}$$

CHAPTER 4

RESULT

4.1 RECIST Definitions of Tumor Response

The chemotherapy treatment effect of the 32 patients was evaluated by the clinical tumor response. The clinical tumor response was classified as complete response (CR), partial response (PR), stable disease (SD) or progressive disease (PD)[17] described as followed:

- Complete response (CR) is defined as the disappearance of all target lesions.
- Partial response (PR) is defined as a $\geq$ 30% decrease in the sum of the longest dimensions of the target lesions taking as a reference the baseline sum longest dimensions.
- Progressive disease (PD) is defined as a $\geq$ 20% increase in the sum of the longest dimensions of the target lesions taking as a reference the smallest sum of the longest dimensions recorded since the treatment started or the appearance of one or more new lesions.
- Stable disease (SD) is defined as neither sufficient shrinkage to quality for PR nor sufficient increase to qualify for PD taking as a reference the smallest sum of the longest dimensions since the treatment started.

In this study, the diameter of the tumor in the 3D HDF Doppler ultrasound images was selected as the target lesions. Patients were classified into two groups: the responder which was classified as CR or PR and the nonresponder which was classified as SD or PD. Table 1 shows the classified catalogue of response of patients. The $D1$, $D2$, $D3$ are the longest diameter of the tumor before chemotherapy measured in the 3D coordinate axis. The experienced physician selected the largest of the three

viewpoints as the starting target lesion and the pathology length of tumor is the ending target lesion. The decrease of the target lesion was calculated by

$$decrease = (\max(D1, D2, D3) - patho\log y) / \max(D1, D2, D3). \quad (9)$$

The number of CR, PR, SD and PD cases was 8, 5, 6 and 3, respectively.

4.3 Simulation Results

The most common means for measuring diagnostic performance for reconstructed images is based on receiver operating characteristic (ROC) analysis with an index of the area (Az) under the ROC curve. The area AZ under the ROC curve is an index of the quantitative measure of overall performance of a diagnostic system. Az value can therefore compare performance using different features to prognose the responses of neo-adjuvant chemotherapy. In this study, the simulation evaluated the vascularity features from both the responder, who was classified as CR or PR, and non-responder, who was classified as SD or PD, groups to identify practical features for tumor angiogenesis. Table 2 shows the changes of result from prior chemotherapy to the first cycle of chemotherapy, and Table 3 shows the changes of result from the first cycle of chemotherapy to the second cycle of chemotherapy. Figure 9, 10 and table 4 shows the Az value of receiver operating characteristic (ROC) curve [18,19] from Table 2 and 3. Based on the Table 2, Table 3, Fig. 9 and Fig. 10, the blood vessels had a tendency to increase from N0 to N1 stage, and had a significant reduction from N1 to N2 stage. The typical vascularization change in chemotherapy responder shows a pattern of initially increasing in vascularity and followed by decreasing in vascularity.

All analyses were made on a single CPU Intel Core i5-750 2.66 GHz personal computer with Microsoft Windows 7 operating system and 8 GB memory. The programs were performed using Matlab 2009a software. Each iteration (including

noise reduction, vascularity centerline extraction and feature extraction) for a single diagnostic 3D HDF Doppler ultrasound imaging data took 20-180 seconds (base on the vascular complexity).

Table 1. The RECIST results of the patients

Patient case #	Tumor Size(CM)				Ratio	
	D1	D2	D3	Pathology	decrease	RECIST
1	4.71	3.01	3.67	2.7	42%	PR
2	3.4	2.25	2.74	2.1	38%	PR
3	2.7	2.16	3.16	2.5	7%	SD
4	2.96	1.46	2.92	0	1	CR
5	2.03	1.41	2.17	2.5	-23%	PD
6	3.9	2.9	4.12	0	100%	CR
7	4.67	1.62	3.84	4	14%	SD
8	4.81	2.19	3.3	0.5	90%	PR
9	4.15	1.64	2.6	4.7	-13%	SD
10	3.08	1.64	2.46	0	100%	CR
11	4.11	2.81	3.37	0.6	85%	PR
12	4.23	1.5	3	1.2	72%	PR
13	2.53	1.56	3.02	1.8	40%	PR
14	4.72	2.92	3.79	2.5	47%	PR
15	4.29	3.42	3.72	3.2	25%	SD
16	3.63	1.72	2.94	1.1	70%	PR
17	3.24	2.56	3.49	0.2	94%	PR
18	3.7	1.71	3.05	2.5	32%	PR
19	1.68	1.6	1.65	0.6	64%	PR
20	2.38	2.44	3.54	4.9	-105%	PD
21	4.03	2.07	3.17	0	100%	CR
22	2.35	2.09	2.55	2.5	-6%	SD
23	2.03	0.99	2.95	2.5	-23%	PD
24	2.85	1.52	2.77	0.8	72%	PR
25	1.9	1.97	1.77	1.5	21%	SD
26	4.12	2.49	2.07	0.8	81%	PR
27	1.41	1.27	1.71	0	100%	CR
28	2.43	1.47	2.29	0	100%	CR
29	2.53	1.24	2.31	0	100%	CR
30	2.67	1.28	1.9	0.2	93%	PR
31	2.61	1.93	1.93	1.5	43%	PR
32	2.82	2.21	3.01	0	100%	CR
Responder:				23		
Nonresponder:				9		
Total:				32		

*The tumor size includes the length of tumors before chemotherapy (D1, D2 and D3) and the pathology length after chemotherapy. The clinical tumor response was classified as CR, PR, SD and PD. Patients were classified into two groups: the responder, which was classified as CR or PR, and the nonresponder, which was classified as SD or PD.

Table 2. The results of features that changed between N0 and N1 stage ((N0-N1)/N0)

Case #	*VI*	*iVI*	*VFI*	*iVFI*	*FI*	*iFI*	*NB*	*NT*	*SDVC*	*DE*	*EN*
1	-1.25	-3.05	-1.55	-3.75	-0.13	-0.17	0.06	0.19	0.76	-0.64	-0.94
2	-12.90	-16.79	-14.35	-17.94	-0.10	-0.06	-28.00	-3.75	0.98	-3.89	-8.71
4	0.41	0.45	0.38	0.39	-0.04	-0.11	0.66	0.59	0.22	0.36	0.40
6	0.27	0.63	-0.03	0.53	-0.41	-0.26	0.27	0.25	-0.15	0.32	0.30
8	0.93	0.96	0.94	0.96	0.10	-0.02	0.94	0.82	-155.11	0.78	0.90
10	-0.82	-0.91	-1.02	-1.10	-0.11	-0.10	0.24	0.40	0.73	-0.65	-0.75
11	-0.95	-1.72	-0.88	-1.28	0.04	0.16	-7.67	-8.00	0.94	-0.75	-0.88
12	0.23	0.29	0.30	0.38	0.09	0.13	0.48	0.18	-2.86	0.17	0.21
13	-0.14	-0.54	-0.20	-0.71	-0.06	-0.11	-1.63	0.00	0.69	-0.28	-0.14
14	-1.02	-0.88	-1.05	-0.92	-0.01	-0.02	-0.83	0.29	0.97	-0.47	-0.79
16	0.20	0.17	0.24	0.25	0.06	0.09	-0.23	-0.60	0.45	0.07	0.15
17	-2.09	-3.19	-2.34	-3.69	-0.08	-0.12	-0.59	0.40	0.92	-0.73	-1.34
18	-1.10	-0.45	-1.25	-0.47	-0.07	-0.01	-1.32	-1.20	0.67	-0.62	-0.91
19	-0.13	-1.30	-0.22	-1.16	-0.08	0.06	0.52	0.50	0.81	0.16	0.01
21	-2.44	-16.57	-2.32	-17.39	0.04	-0.05	-4.00	-0.80	0.90	-1.63	-2.22
24	-0.89	-0.79	-0.99	-0.86	-0.06	-0.04	-0.57	0.46	0.70	-0.48	-0.71
26	-0.46	-0.97	-0.40	-0.93	0.04	0.02	-0.50	0.13	-5.63	-0.25	-0.35
27	-1.38	-1.54	-1.26	-1.42	0.05	0.05	0.20	0.67	0.44	-0.57	-0.99
28	-0.36	0.67	-0.11	0.74	0.18	0.21	0.27	0.22	-0.45	-0.36	-0.38
29	0.21	0.40	0.23	0.48	0.03	0.14	0.05	0.08	0.66	0.11	0.18
30	0.09	0.43	0.07	0.43	-0.02	-0.01	0.13	0.50	-4.77	0.03	0.06
31	-0.01	0.02	0.01	0.05	0.02	0.03	0.17	0.23	-2.60	0.00	0.01
32	-1.27	-1.73	-1.12	-1.55	0.06	0.07	-1.03	-0.46	0.73	-0.42	-0.84
3	0.24	0.32	-0.01	0.07	-0.33	-0.38	0.37	0.16	-0.65	0.08	0.17
5	-0.11	-0.29	-0.25	-0.49	-0.13	-0.16	-0.07	-0.20	0.24	0.04	-0.06
7	0.78	0.75	0.78	0.76	0.00	0.02	0.45	0.58	-1.87	0.47	0.69
9	-0.23	-0.32	-0.29	-0.37	-0.05	-0.04	-0.22	-0.08	-1.20	-0.20	-0.21
15	0.78	0.80	0.78	0.80	0.01	-0.02	0.71	0.86	-1897.00	0.61	0.72
20	0.30	0.34	0.32	0.40	0.03	0.09	0.37	0.23	0.03	0.26	0.29
22	0.10	0.10	0.09	0.07	-0.02	-0.03	-0.04	-0.09	-12.06	0.10	0.10
23	-0.33	-0.08	-0.26	-0.04	0.05	0.04	0.22	0.13	-0.19	-0.07	-0.20
25	0.41	0.59	0.51	0.66	0.18	0.19	-4.00	-1.00	-0.53	0.24	0.35

*The white region is the responders and the gray region is the no-responders

Table 3. The results of features that changed between N1 and N2 stage ((N1-N2)/N1)

Case #	*VI*	*iVI*	*VFI*	*iVFI*	*FI*	*iFI*	*NB*	*NT*	*SDVC*	*DE*	*EN*
1	0.64	0.68	0.66	0.70	0.06	0.05	0.39	-0.06	-2.72	0.38	0.54
2	0.65	0.58	0.66	0.59	0.03	0.03	0.78	0.53	-6.83	0.45	0.59
4	0.47	0.45	0.50	0.50	0.06	0.09	0.46	0.00	-1.80	0.30	0.41
6	0.92	0.80	0.93	0.80	0.17	0.00	0.96	0.83	-0.89	0.83	0.89
8	0.58	0.69	0.65	0.75	0.16	0.19	0.79	0.40	-0.13	0.47	0.55
10	0.09	0.90	0.46	0.94	0.41	0.37	0.00	-1.67	-0.71	0.06	0.07
11	0.50	0.67	0.51	0.68	0.04	0.03	0.50	0.67	-14.19	0.38	0.45
12	-0.07	-0.21	-0.29	-0.67	-0.21	-0.38	0.83	0.78	-0.33	0.05	-0.02
13	0.57	0.76	0.65	0.83	0.18	0.28	0.67	0.00	-2.22	0.40	0.50
14	0.47	0.37	0.47	0.36	-0.01	-0.01	0.44	0.00	-4.91	0.24	0.39
16	0.42	0.50	0.43	0.50	0.02	-0.01	0.86	0.50	0.27	0.39	0.42
17	0.56	0.63	0.60	0.69	0.09	0.16	0.38	-0.50	-3.92	0.33	0.46
18	-0.49	-0.93	-0.44	-0.99	0.03	-0.03	0.08	0.36	-0.87	-0.19	-0.36
19	-0.11	-0.63	0.03	-0.45	0.13	0.11	0.31	-0.67	0.64	-0.11	-0.09
21	1.00	1.00	1.00	1.00	1.00	1.00	1.00	1.00	-294.39	1.00	1.00
24	0.28	0.25	0.33	0.30	0.07	0.07	0.03	0.29	0.45	0.17	0.24
26	0.41	0.21	0.36	0.17	-0.07	-0.06	0.58	0.00	0.91	0.23	0.33
27	0.99	0.98	0.99	0.98	0.17	0.15	0.98	0.80	-14.46	0.95	0.98
28	0.88	0.99	0.88	1.00	-0.05	0.20	0.82	0.86	0.37	0.86	0.88
29	0.87	0.99	0.89	0.99	0.18	0.17	0.95	0.92	-5.98	0.78	0.84
30	0.65	0.38	0.72	0.50	0.19	0.20	0.55	0.00	0.90	0.59	0.63
31	0.35	0.38	0.39	0.41	0.05	0.04	0.10	-1.00	-1.39	0.10	0.21
32	0.37	0.56	0.33	0.55	-0.05	-0.04	0.52	-0.21	0.31	0.14	0.27
3	0.00	0.00	-0.02	0.02	-0.02	0.03	-0.59	0.00	-0.90	0.05	0.01
5	0.03	0.07	-0.05	0.01	-0.09	-0.07	0.39	0.67	-0.39	0.18	0.09
7	-0.68	-0.84	-0.79	-0.97	-0.07	-0.07	0.00	0.00	0.94	-0.35	-0.57
9	0.55	0.57	0.55	0.58	0.00	0.01	0.61	0.38	0.52	0.41	0.49
15	-2.50	-3.66	-2.70	-3.72	-0.06	-0.01	-1.17	-4.67	0.95	-1.29	-2.05
20	-0.17	-0.90	-0.14	-1.12	0.03	-0.12	-0.32	-0.20	0.52	-0.18	-0.18
22	0.26	0.30	0.26	0.30	0.00	0.00	0.20	-0.58	-0.11	0.16	0.22
23	0.22	0.14	0.27	0.18	0.06	0.05	0.41	0.38	-0.36	0.20	0.22
25	-0.32	-0.70	-0.59	-1.12	-0.21	-0.24	0.40	0.50	0.30	-0.02	-0.20

*The white region is the responders and the gray region is the no-responders

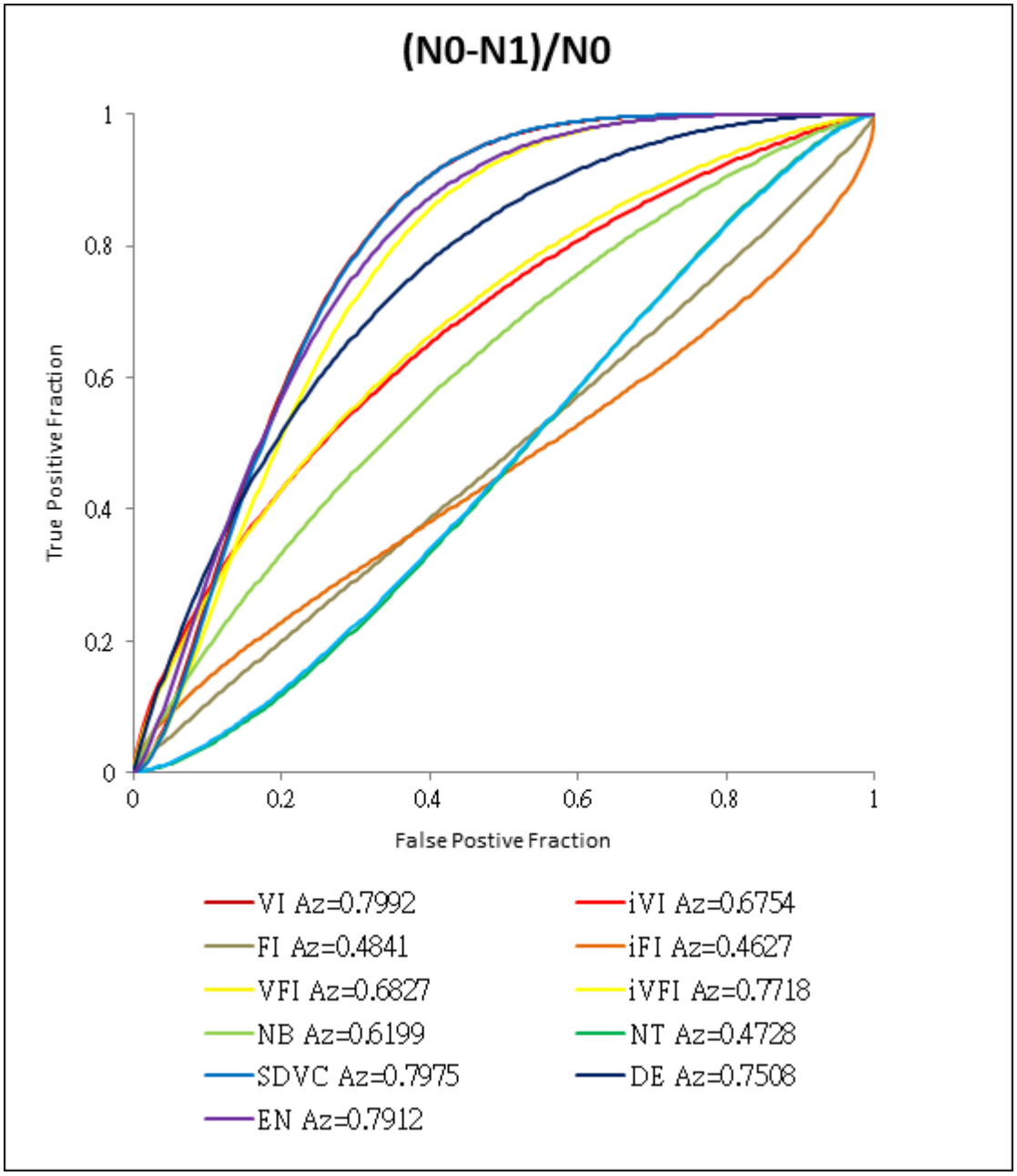

Figure 9. The result of ROC curve from Table 2

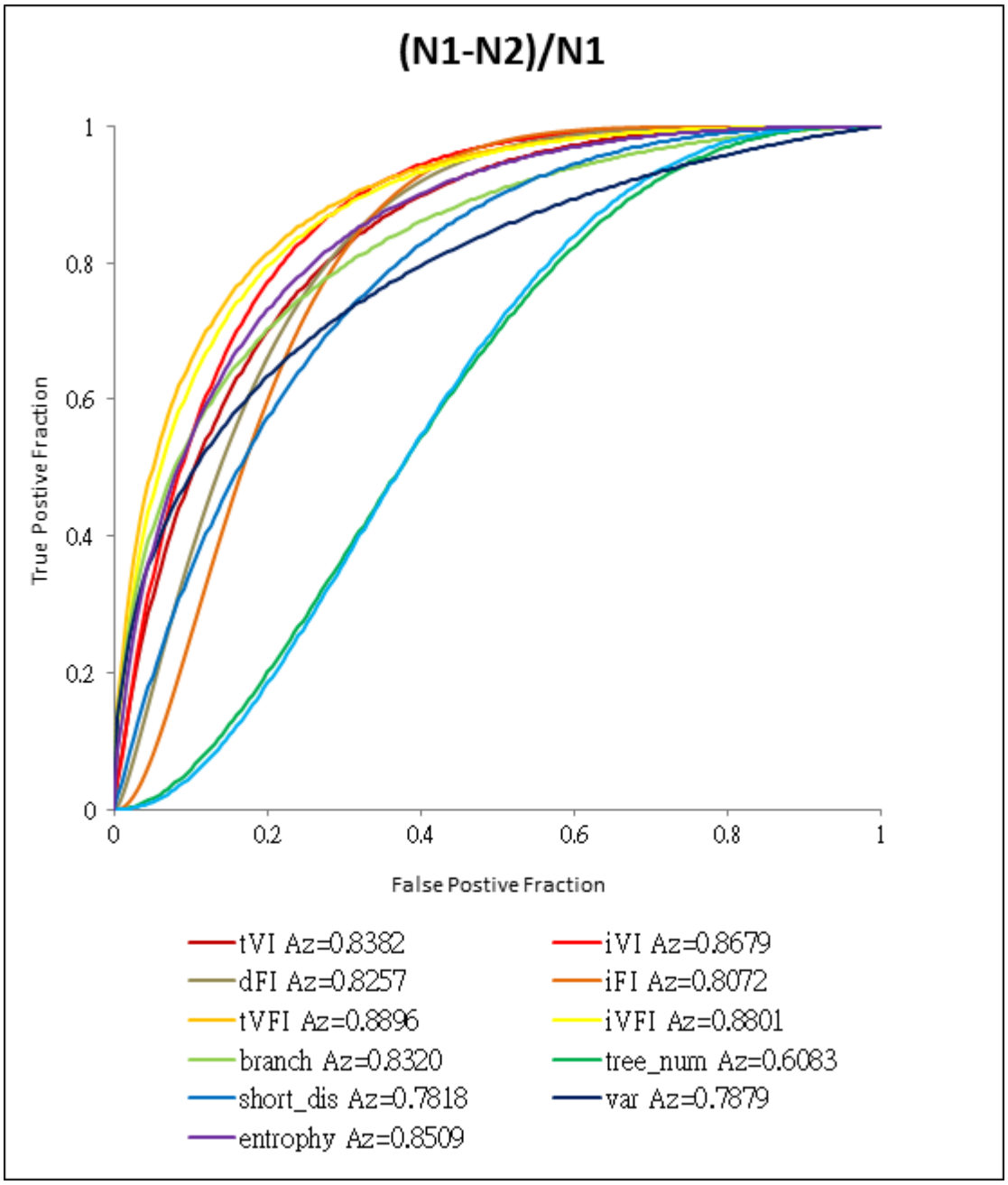

Figure 10. The ROC curve result from Table 3

Table 4. The results of ROC curve

	(N0-N1)/N0	(N1-N2)/N1
VI	0.799	0.838
iVI	0.675	0.868
FI	0.484	0.826
iFI	0.463	0.807
VFI	0.683	0.890
iVFI	0.772	0.880
NB	0.620	0.832
NT	0.473	0.608
SDVC	0.798	0.782
DE	0.751	0.788
EN	0.791	0.851

CHAPTER 5

DISCUSSION and CONCLUSION

Over the last decade, the use of neo-adjuvant chemotherapy has emerged as the standard of medical care for patients with locally advanced breast cancer. However, two large randomized trials proved that the survival rates of advanced breast cancer were equivalent in patients receiving preoperative or postoperative chemotherapy [20,21]. The shortcoming of current clinical practice is time consuming because the decision making is based on the pathologic response at the end of chemotherapy. The features *VI*, *iVFI*, *NB*, *DE* and *EN* had be noticed that had increasing trends, and *SDVC* was closed to the center of mass with the initiation of neo-adjuvant chemotherapy to period 1. Followed by period 1 to period 2, features *VI*, *iVI*, *FI*, *iFI*, *VFI*, *iVFI*, *NB* and *EN* had decreased significantly. Figure 11 shows the vascular changes in period (N0-N2) from a responder case. Moreover, Table 4 supports the values of features from this case. The thesis postulated that after initiation of chemotherapy, abundant angiogenic factors such as vascular endothelial growth factor (VEGF), releasing from apoptotic and necrotic breast cancer cells, resulted in increasing vascularity profoundly. After peak vascularity, the blood vessels decreased gradually at a later stage of chemotherapy because of fewer angiogenic factors released by the remaining tumor cells that are chemotherapy sensitive. The results (Table 3 and Fig. 10) indicated that the features *VI*, *iVI*, *FI*, *iFI*, *VFI*, *iVFI*, *NB* and *EN* as potential early predictors (in period N1-N2) for good responses to neo-adjuvant chemotherapy.

The point of view of classification features for cases had good response, *VI* had superior changes whenever the period of N0-N1 or N1-N2. All the quantization features had a substantial reduction at N1-N2 stage. In the vascular directional

characteristics suggested (*DE* and *EN*) the Az values did not have considerable performance in the ROC curve. According to the Az values, the vascular directional features had smooth changes either in the period of N0-N1 or N1-N2. Furthermore, the morphological characteristics of number of vascular trees *NT* had not good response in our researches. On the other hand, *NB* had a good response in N1-N2 (Az = 0.832), and we observed blood vessels closed (N0-N1) then away (N1-N2) from the barycenter of tumor by *SDVC*. Figure 12 shows the broken line graph (values from table 5), and all the values is defined as 1 at N0, N1/N0 at N1 and N2/N1 at N2.

Collectively, this study has demonstrated that vascularity changes from the cases of the neo-adjuvant chemotherapy using 3D HDF power Doppler ultrasound imaging. The tendencies and peaks of the vascularization features seem to be useful information for physicians to forecast the effects of chemotherapy treatments. Early prediction using the 3D HDF power Doppler ultrasound could diminish the unnecessary chemotherapy treatments for the patient whose poor response to certain chemotherapy strategies. Thus, it is suggested more cases and more features in the future will be helpful to increase prediction accuracy.

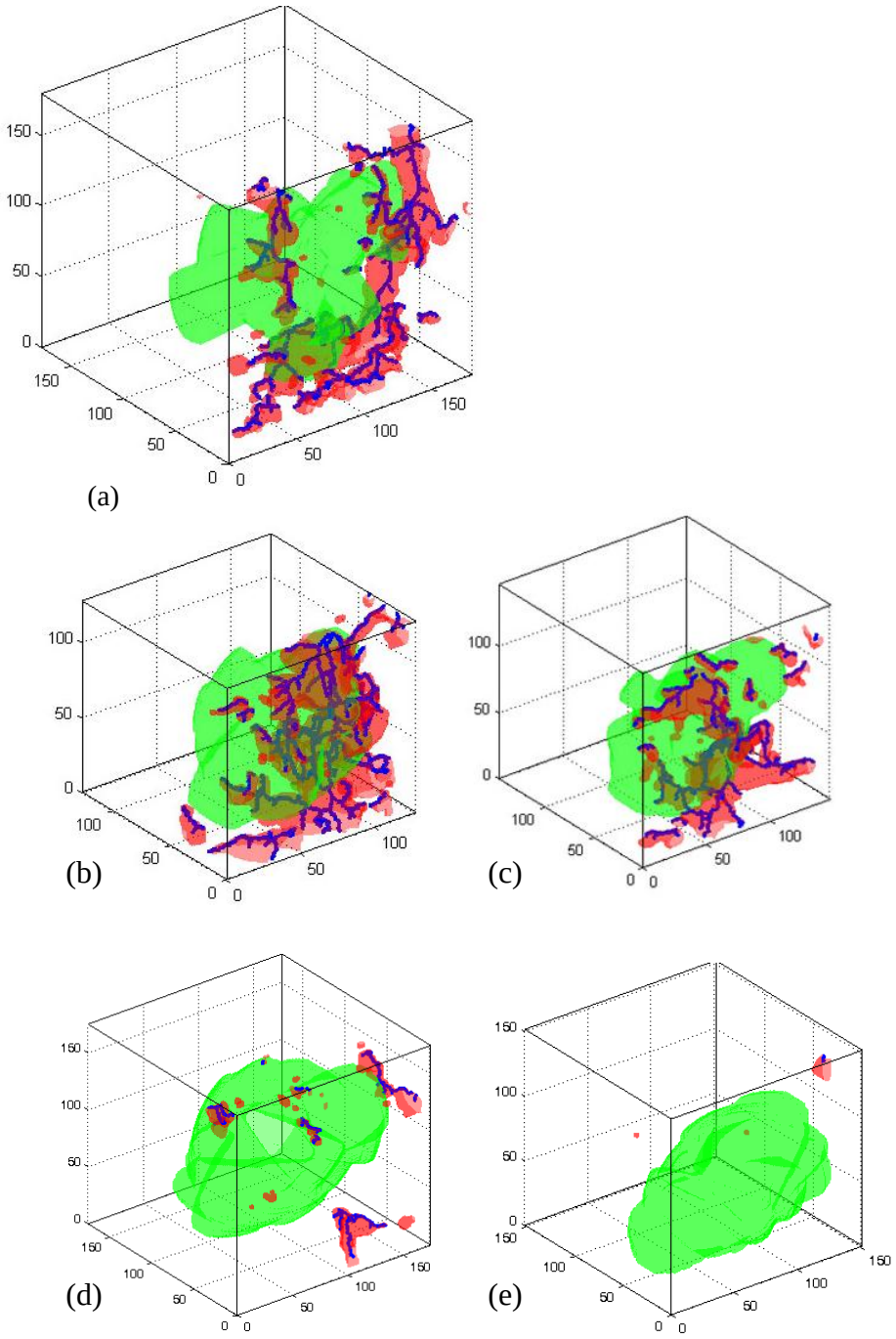

Figure 11. The vascular changes from a responder case (case#17) at period (a) N0; (b) N1; (c) N2; (d) N3; (e) N4

Table 5. The values of features on figure 11

	N0	N1	N2	N3	N4
VI	0.03	0.08	0.04	0.03	0
iVI	0.01	0.05	0.02	0	0
VFI	1.62	5.42	2.17	0.16	0
iVFI	0.71	3.33	1.04	0.05	0
FI	62.4	67.31	61.39	5.33	0
iFI	61.21	68.47	57.25	50	0
NB	82	130	80	13	1
NT	10	6	9	4	1
SDVC	620	50	246	2957	48350
DE	9559.43	16532.19	11090.4	1313.72	37.98
EN	0.16	0.38	0.21	0.02	0

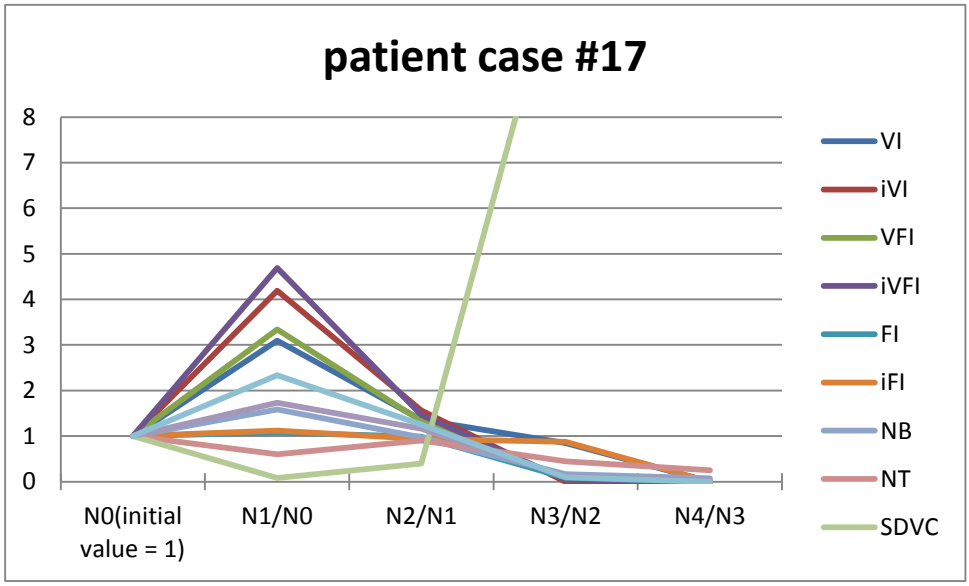

Figure 12. The values of features change from a responder case (case#17)

Acknowledgment

This research was supported by National Science Council of the Republic of China (Taiwan) under Contract No. NSC99-2221-E-029 -031.

References

[1] I.E. Smith, "Neoadjuvant/presurgical treatments," *Breast Cancer Res.*, vol. 10 Suppl 4 pp. S24, 2008.

[2] J. Folkman, "Tumor angiogenesis," *Adv. Cancer Res.*, vol. 43 pp. 175-203, 1985.

[3] J. Folkman, "What is the evidence that tumors are angiogenesis dependent?," *J. Natl. Cancer Inst.*, vol. 82, no. 1, pp. 4-6, Jan. 1990.

[4] H.M. Al-Otum, "Morphological operators for color image processing based on Mahalanobis distance measure," *Optical Engineering*, vol. 42, no. 9, pp. 2595-2606, Sept. 2003.

[5] R.C. Gonzalez and R.E. Woods, *Digital Image Processing*, third ed. 2010.

[6] K. Palagyi and A. Kuba, "A 3D 6-subiteration thinning algorithm for extracting medial lines," *Pattern Recognition Letters*, vol. 19, no. 7, pp. 613-627, May 1998.

[7] N.J. Raine-Fenning, B.K. Campbell, J.S. Clewes, N.R. Kendall, and I.R. Johnson, "The reliability of virtual organ computer-aided analysis (VOCAL) for the semiquantification of ovarian, endometrial and subendometrial perfusion," *Ultrasound Obstet. Gynecol.*, vol. 22, no. 6, pp. 633-639, Dec. 2003.

[8] N.J. Raine-Fenning, J.S. Clewes, N.R. Kendall, A.K. Bunkheila, B.K. Campbell, and I.R. Johnson, "The interobserver reliability and validity of volume calculation from three-dimensional ultrasound datasets in the in vitro setting," *Ultrasound Obstet. Gynecol.*, vol. 21, no. 3, pp. 283-291, Mar. 2003.

[9] R.A. Haddad and A.N. Akansu, "A class of fast Gaussian binomial filters for speech and image processing," *IEEE Transactions on Acoustics, Speech and Signal Processing*, vol. 39, no. 3, pp. 723-727, Mar. 19910.

[10] S.F. Huang, R.F. Chang, W.K. Moon, Y.H. Lee, D.R. Chen, and J.S. Suri, "Analysis of tumor vascularity using three-dimensional power Doppler ultrasound images," *IEEE Trans. Med. Imaging*, vol. 27, no. 3, pp. 320-330, Mar. 2008.

[11] R. Webster, M. Harris, R. Shenk, J. Blumenstock, J. Gerber, C. Billman et al., "Using an approximation to the euclidean skeleton for efficient collision detection and tissue deformations in surgical simulators," *Stud. Health Technol. Inform.*, vol. 111 pp. 596-598, 2005.

[12] N.D. Cornea, D. Silver, and P. Min, "Curve-skeleton properties, applications, and algorithms," *IEEE Transactions on Visualization and Computer Graphics*, vol. 13, no. 3, pp. 530-548, May 2007.

[13] C. Lohou and J. Dehos, "Automatic correction of Ma and Sonka's thinning algorithm using P-simple points," *IEEE TRANSACTIONS ON PATTERN ANALYSIS AND MACHINE INTELLIGENCE*, vol. 32, no. 6, pp. 1148-1156, June 2010.

[14] Chris Pudney, "Distance-Based Skeletonization of 3D Images," *IEEE TENCON - Digital Signal Processing Applications*, pp. 209-214, 1996.

[15] I.Y. Jarvela, P. Sladkevicius, S. Kelly, K. Ojha, G. Nargund, and S. Campbell, "Three-dimensional sonographic and power Doppler characterization of ovaries in late follicular phase," *Ultrasound Obstet. Gynecol.*, vol. 20, no. 3, pp. 281-285, Sept. 2002.

[16] W.H. Kuo, C.N. Chen, F.J. Hsieh, M.K. Shyu, L.Y. Chang, P.H. Lee et al., "Vascularity change and tumor response to neoadjuvant chemotherapy for advanced breast cancer," *Ultrasound Med. Biol.*, vol. 34, no. 6, pp. 857-866, June 2008.

[17] M.J. Byrne and A.K. Nowak, "Modified RECIST criteria for assessment of response in malignant pleural mesothelioma," *Annals of Oncology*, vol. 15, no. 2, pp. 257-260, Feb. 2004.

[18] J.A. Hanley and B.J. McNeil, "The meaning and use of the area under a receiver operating characteristic (ROC) curve," *Radiology*, vol. 143, no. 1, pp. 29-36, Apr. 1982.

[19] J.A. Hanley, "Receiver operating characteristic (ROC) methodology: the state of the art," *Crit Rev. Diagn. Imaging*, vol. 29, no. 3, pp. 307-335, 1989.

[20] E.P. Mamounas, "Overview of National Surgical Adjuvant Breast Project neoadjuvant chemotherapy studies," *Semin. Oncol.*, vol. 25, no. 2 Suppl 3, pp. 31-35, Apr. 1998.

[21] P.C. Clahsen, C.J. van de Velde, J.P. Julien, J.L. Floiras, T. Delozier, F.Y. Mignolet et al., "Improved local control and disease-free survival after perioperative chemotherapy for early-stage breast cancer. A European Organization for Research and Treatment of Cancer Breast Cancer Cooperative Group Study," *J. Clin. Oncol.*, vol. 14, no. 3, pp. 745-753, Mar. 1996.